

Bioinformatics-based screening of hub genes for prostate cancer bone metastasis and analysis of immune infiltration

Shu-Kun Lin, MMed^a , Chen-Ming Zhang, MD^a, Bo Men, MBBS^{a,*}, Zhong Hua, MD^a, Si-Cheng Ma, MMed^a, Fang Zhang, MD^a

Abstract

Bioinformatics analysis of genes and immune cells that influence prostate cancer (PCa) bone metastases. Using the gene expression omnibus database, we analyzed a PCa bone metastasis dataset. Differentially expressed genes were identified through the utilization of GEO2R and weighted gene co-expression network analysis. Gene set enrichment analysis software was used to identify important pathways. In addition to creating a network of protein–protein interactions, functional enrichment analyses were conducted using Kyoto encyclopedia of genes databases. To screen hub genes, Cytoscape software was used with the CytoHubba plug-in and performed mRNA and survival curve validation analysis of key genes using the cBioPortal website and GEPIA2 database. Immune infiltration analysis was performed using the CIBERSORTx website, and finally, immune cell correlation analysis was performed for key genes according to the TIMER database. A total of 197 PCa bone metastasis risk genes were screened, “G2M_CHECKPOINT” was significantly enriched in PCa bone metastasis samples according to genomic enrichment analysis. Based on the protein interactions network, we have identified 10 alternative hub genes, and 3 hub genes, CCNA2, NUSAP1, and PBK, were validated by the cBioPortal website and the GEPIA2 database. T cells regulatory and macrophages M0 may influence PCa to metastasize to bones, according to CIBERSORTx immune cell infiltration analysis. TIMER database analysis found different degrees of correlation between 3 key genes and major immune cells. PCa bone metastasis has been associated with CCNA2, NUSAP1, and PBK. T cells regulatory and macrophages (M0) may also be involved.

Abbreviations: DEGs = differentially expressed genes, GSEA = gene set enrichment analysis, PCa = prostate cancer, PPI = protein–protein interaction networks, Tregs = regulatory T cells, WGCNA = weighted gene co-expression network analysis.

Keywords: bioinformatics, differentially expressed gene, immune infiltration, prostate cancer bone metastasis, WGCNA

1. Introduction

Men's health is seriously threatened by prostate cancer (PCa), which is the second most common malignant tumor.^[1] The main treatment option for hormone-sensitive prostate tumors with distant metastases is androgen deprivation therapy. Nonetheless, this carcinoma inevitably develops into castration-resistant PCa, characterized by an increased tendency for distant metastasis in the tumor cells.^[2] Predominantly, PCa metastasizes to the bone, which serves as the primary source of morbidity.^[3] The ^{99m}Tc-MDP bone scan is a common method of diagnosing PCa bone metastases.^[4] However, its specificity remains unsatisfactory. Further elucidation of bone metastasis mechanisms in PCa is needed, and the exploration of novel biomarkers. Such endeavors aim to provide additional support for clinical diagnosis and treatment.

Prior research into tumor pathogenesis has shown that immune evasion is a significant element in the development of malignancy.^[5] Through interactions with tumor cells, different phenotypes of tumor-associated immune cells can either promote or hinder tumor growth, as a result of the inflammatory milieu, immune cells may contribute to PCa spread.^[6] Recent investigations underscore the significant roles tumor-associated immune cells play in initiating, progressing, and metastasizing PCa.^[7] Therefore, immunology studies of PCa bone metastases hold the potential to provide valuable insights and future treatment strategies.

Bioinformatics, an interdisciplinary field, has seen extensive use in unveiling the molecular mechanisms underlying diseases.^[8] Using scale-free networks, weighted gene co-expression network analysis (WGCNA) visualizes the interactions

National Undergraduate Innovation and Entrepreneurship Training Program Project (202210471022, 202310471011).

All authors are agreed.

The authors have no conflicts of interest to disclose.

The datasets generated during and/or analyzed during the current study are publicly available.

This article does not contain any studies with human participants the authors.

^a The Second Clinical Medical College of Henan University of Traditional Chinese Medicine, Zhengzhou, Henan, China.

* Correspondence: Bo Men, The Second Clinical Medical College of Henan University of Traditional Chinese Medicine, Zhengzhou, Henan 450002, China (e-mail: 18625507662@163.com).

Copyright © 2024 the Author(s). Published by Wolters Kluwer Health, Inc. This is an open-access article distributed under the terms of the Creative Commons Attribution-Non Commercial License 4.0 (CCBY-NC), where it is permissible to download, share, remix, transform, and build up the work provided it is properly cited. The work cannot be used commercially without permission from the journal.

How to cite this article: Lin S-K, Zhang C-M, Men B, Hua Z, Ma S-C, Zhang F. Bioinformatics-based screening of hub genes for prostate cancer bone metastasis and analysis of immune infiltration. *Medicine* 2024;103:46(e40570).

Received: 28 December 2023 / Received in final form: 27 September 2024 /

Accepted: 30 October 2024

<http://dx.doi.org/10.1097/MD.0000000000040570>

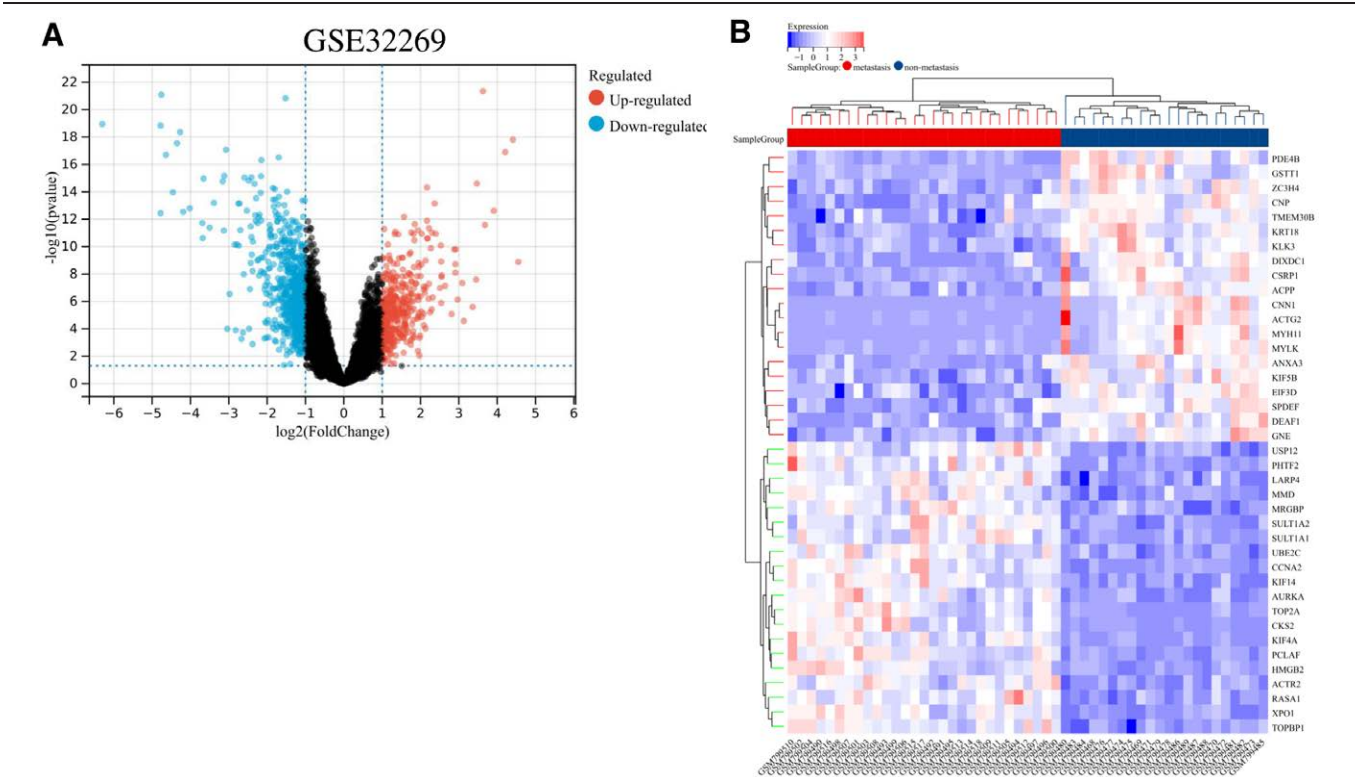


Figure 1. A volcano plot and heat map showing differentially expressed mRNAs. (A) Volcano graphic showing the GSE32269 dataset's DEGs; (B) heat map of the top 40 DEGs. DEGs = differentially expressed genes.

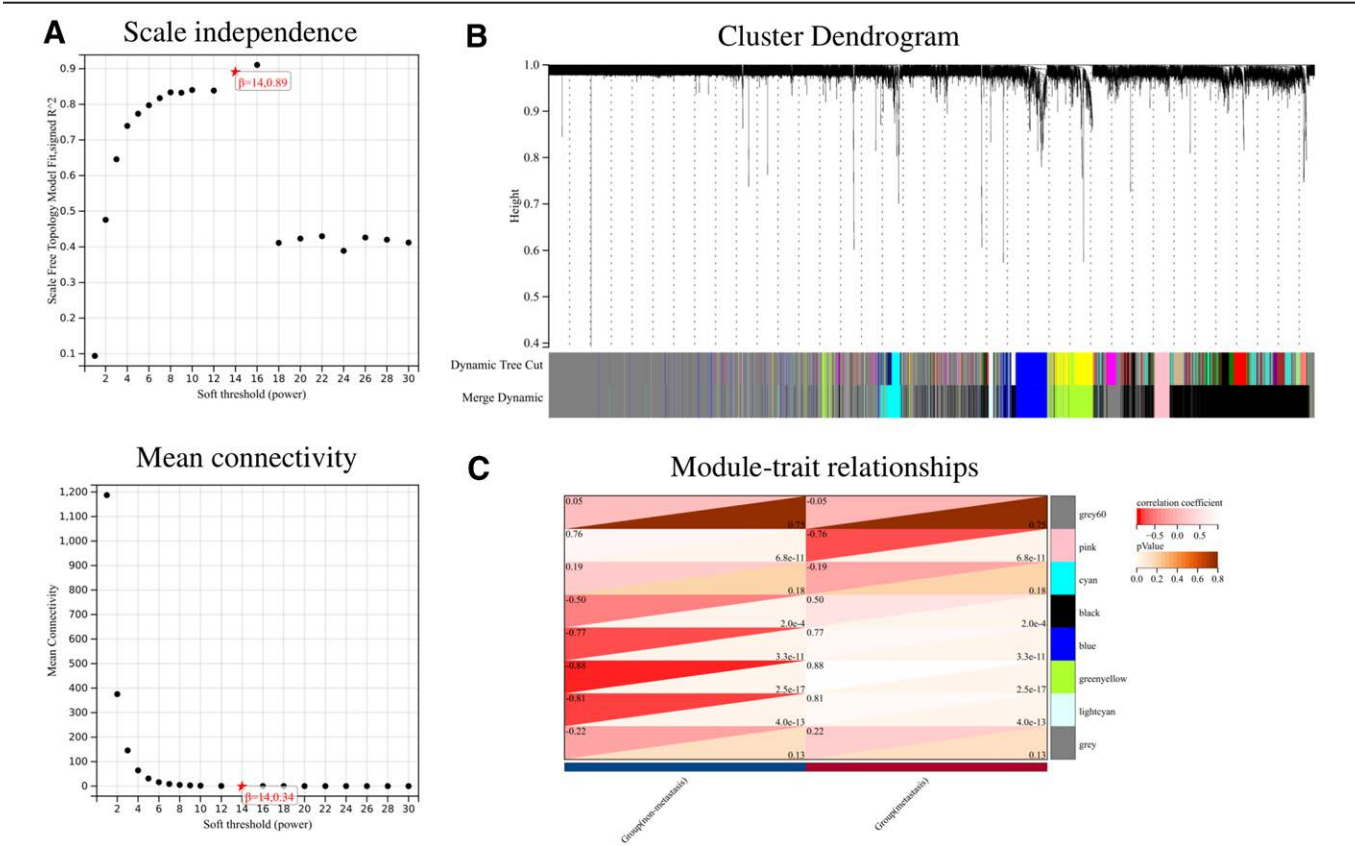


Figure 2. Co-expression module analysis of WGCNA based on GSE32269. (A) Analyzing scale-free fit indexes under different soft threshold powers ($\beta = 14$); (B) gene clustering dendrogram (different colors represent different modules); (C) correlation analysis of each module with bone metastasis of prostate cancer.

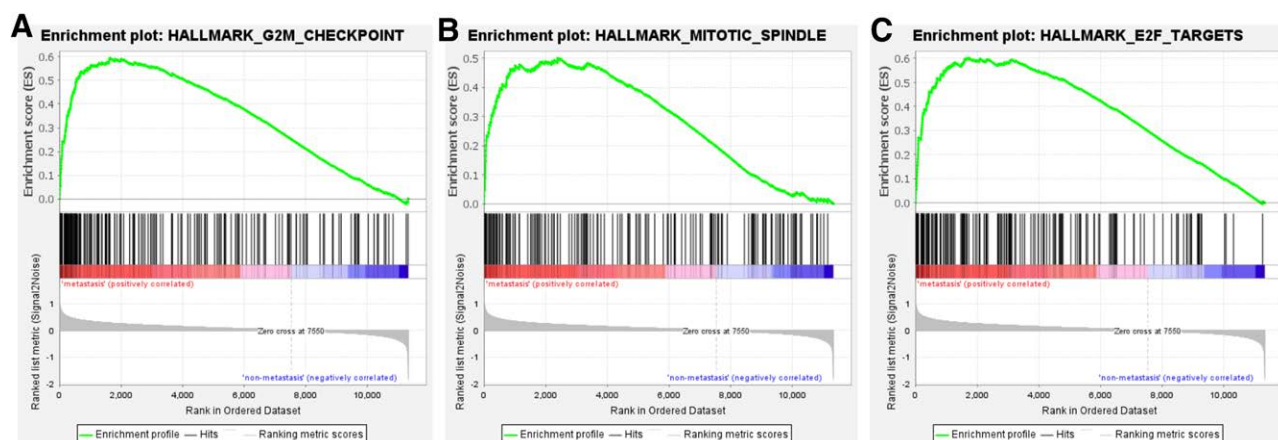


Figure 3. Results of gene set enrichment analysis. (A) Enrichment plot for G2M_CHECKPOINT, $|NES|=1.81$, $FDR = 0.15$, $P = .01$. (B) Enrichment plot for MITOTIC_SPINDLE, $|NES|=1.76$, $FDR = 0.12$, $P = .01$. (C) Enrichment map of E2F_TARGETS, $|NES|=1.65$, $FDR = 0.18$, $P < .05$.

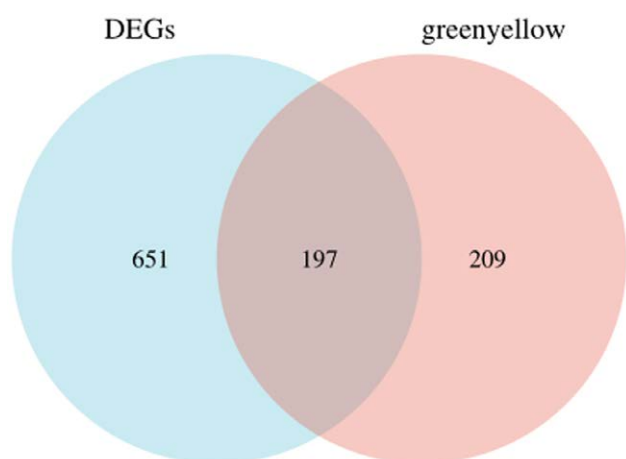


Figure 4. Differently expressed genes take intersection with greenyellow module.

among various components of a biological system, Significantly, WGCNA has emerged as a potential technique for finding new biological tumor markers.^[9]

2. Materials and methods

2.1. Obtaining and processing data

The PCa mRNA dataset GSE32269 was downloaded from the gene expression omnibus database,^[10] A total of 22 samples were collected from localized primary PCas and 29 from bone metastases associated with PCa.

2.2. Identification of candidate differentially expressed genes (DEGs)

We screened the mRNA dataset GSE32269 using the online tool GEO2R with the screening criteria being $\text{adj-}P < 0.05$ and $|\log FC| \geq 1$. We demonstrated DEGs with a volcano plot, additionally, a heat map was used to display the distinct expression patterns of the top 40 genes that exhibited differential expression in every sample.

2.3. WGCNA analysis and module gene selection

The matrix data of GSE32269, performed sample was clustered through the online tool Sanger Box,^[11] defined the similarity

matrix of gene co-expression, calculated the soft threshold to determine the adjacency function of gene network formation, a topology overlap matrix was created by converting the similarity matrix into an adjacency matrix, then by calculating the dissimilarity between nodes. The dynamic cut tree method was used to divide genes into different modules and color them differently. For further study, we chose genes from the module with the highest link to PCa bone metastases.

2.4. Gene set enrichment analysis (GSEA) pathway analysis

Patients with PCa bone metastases and controls were analyzed using GSEA to determine whether pathways were statistically enriched.^[12] The screening criteria for enriched pathways were $|NES| > 1$, $P < .05$, $FDR < 0.25$.

2.5. Screening of high-risk DEGs

Disease-causing genes common to the modules and differentially expressed genes screened by GEO2R were obtained according to the Venn Diagram method.

2.6. Functional enrichment analyses

Using the DAVID database, gene ontology and Kyoto encyclopedia of genes and genomes enrichment analyses were conducted for high-risk differentially expressed genes,^[13] setting the species as *Homo sapiens* (*Homo sapiens*), and using $P < .05$ as the screening criterion.

2.7. Construction of protein–protein interaction networks (PPI) network

Using the String database, we constructed the intergenic protein interaction network,^[14] the minimum confidence level was established > 0.4 . Cytoscape software has the function of network visualization and analysis, the cytoHubba plug-in has built-in multiple topology analysis algorithms, and in this study, A Maximum Clique Centrality topology algorithm was used to rank the nodes in the PPI network, and the top 10 genes were considered hub genes.

2.8. Hub gene validation and survival analysis

The cBioPortal^[15] database can be used for a wide range of cancer genomics, in order to screen for pivotal genes, there must be a statistically significant difference in expression between samples from

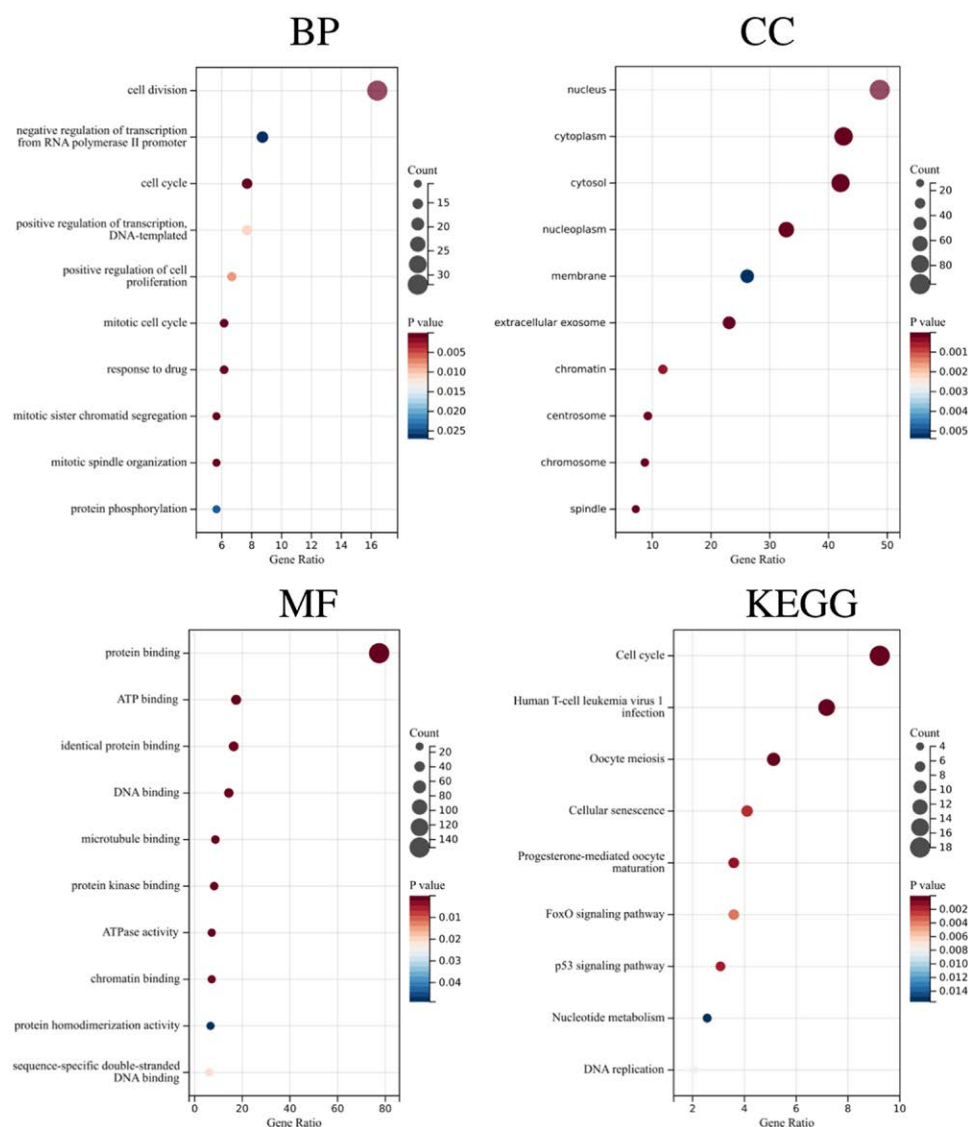


Figure 5. Analysis of DEGs based on GO and KEGG enrichment. DEGs = differentially expressed genes, GO = gene ontology, KEGG = Kyoto encyclopedia of genes and genomes.

primary PCas and those from bone metastases of PCa ($P < .05$). GEPIA2^[16] is an analytical website developed based on the UCSC Xena program, At $P < .05$, GEPIA2 was statistically significant in analyzing survival prognoses for the pivotal genes in this study.

2.9. Detection of immune infiltration

An inverse convolution algorithm is utilized by CIBERSORTx to measure immune cell infiltration levels in samples.^[17] In this study, simulations were set to 500 calculations, using the Wilcoxon test, PCa patients with bone metastases and those with non-metastases were compared for immune cell infiltration, then analyze the relationship between hub genes and immune cells in the TIMER database.^[18] In order to qualify for this study, $P < .05$ had to be met.

3. Results

3.1. Candidate DEGs identification

In total, 848 differentially expressed genes were identified (Fig. 1).

3.2. Key modules for WGCNA analysis and screening

The original dataset of GSE32269 was preprocessed using the SangerBox online analysis website for probing, gene name conversion, normalization, etc. After deleting unrecognizable and duplicated genes, a total of 11,343 genes were obtained. The scale-free fitting index R^2 of 0.89 led to the determination of a soft threshold = 14 (Fig. 2A). Module merging threshold was set at 0.25, a minimum number of genes in modules was 30, lastly, 8 modules were formed (Fig. 2B). According to the correlation calculation, the green-yellow module was positively associated with PCa bone metastasis. ($\text{cor} = 0.88$, $P = 2.5e-17$) (Fig. 2C). There are 406 genes within the green-yellow module.

3.3. GSEA pathway analysis

Gene expression data from PCa bone metastasis patients were analyzed using GSEA software. The results showed 3 gene sets were significantly enriched at $\text{FDR} < 25\%$. They are G2M_CHECKPOINT; MITOTIC_SPINDLE; and E2F_TARGETS, respectively (Fig. 3).

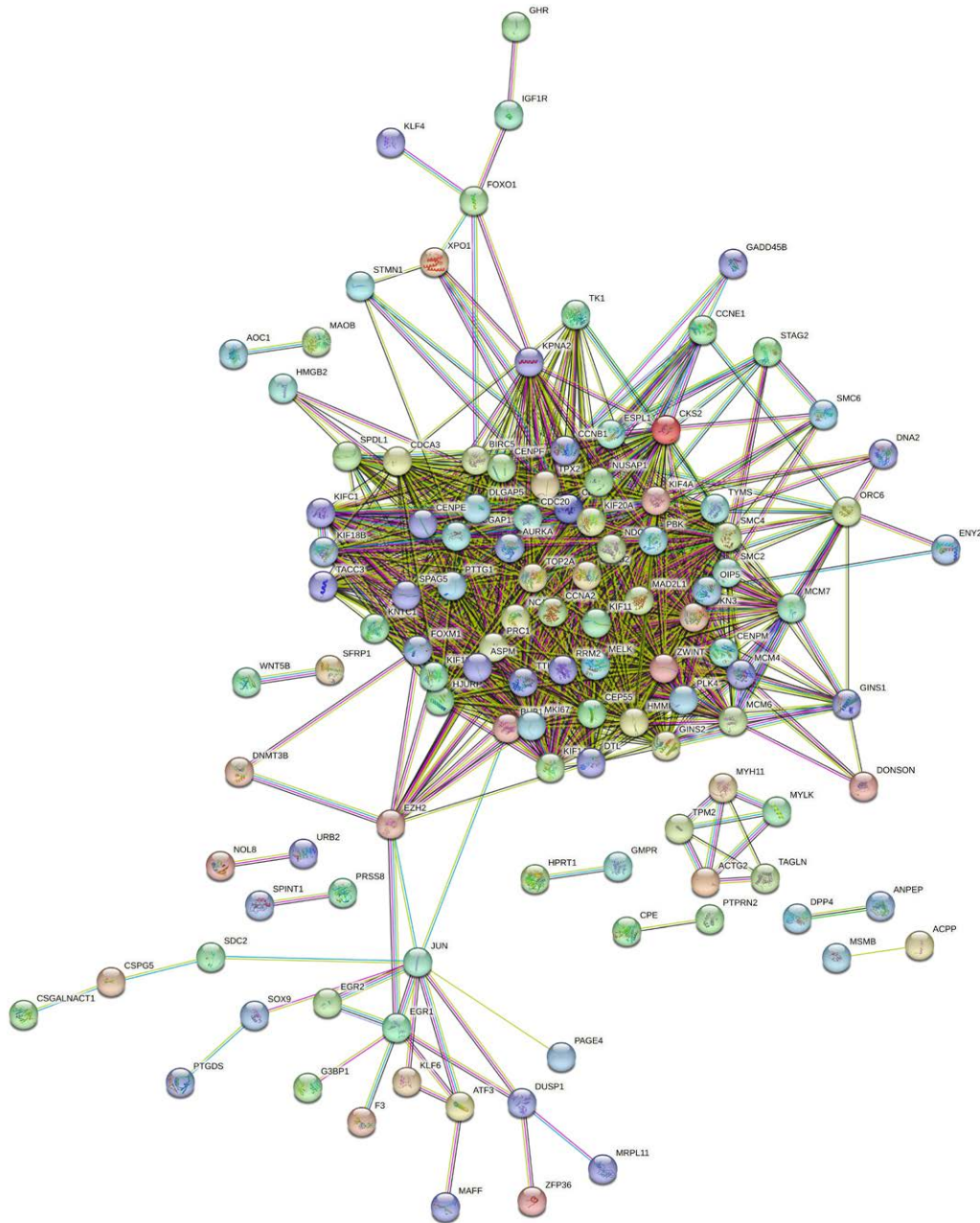


Figure 6. PPI network of high-risk differentially expressed genes. PPI = protein–protein interaction networks.

3.4. Screening of high-risk DEGs

The green-yellow module obtained by WGCNA analysis contained 406 genes, and 848 differentially expressed genes were obtained by $\text{adj-}P < .05, |\log\text{FC}| \geq 1$. The intersection was taken by the Venn Diagram method, and 197 genes were finally obtained (Fig. 4).

3.5. Functional enrichment analyses

Biological processes such as cell division, cellular components such as the nucleus, and molecular functions such as protein binding were most enriched in the genes. Based on Kyoto encyclopedia of genes and genomes pathway enrichment analysis, these genes are predominantly associated with cell cycle pathways (Fig. 5).

3.6. Construction of PPI network

The String database is used to construct a protein interaction network between differentially expressed genes (Fig. 6). Top 10 ranked hub genes were determined using CytoHubba's Maximum Clique Centrality topology algorithm after downloading and importing protein interaction files, which were RACGAP1, NUSAP1, ASPM, CDK1, AURKA, CCNA2, PBK, DLGAP5, KIF4A, and NCAPG.

3.7. Validation of hub genes and survival analysis

CCNA2, NUSAP1, and PBK were the 3 pivotal genes that met the criteria. Comparing bone metastatic PCa samples to primary PCa samples, CCNA2, NUSAP1, and PBK were all upregulated (Fig. 7), and Kaplan–Meier survival analyses suggest that

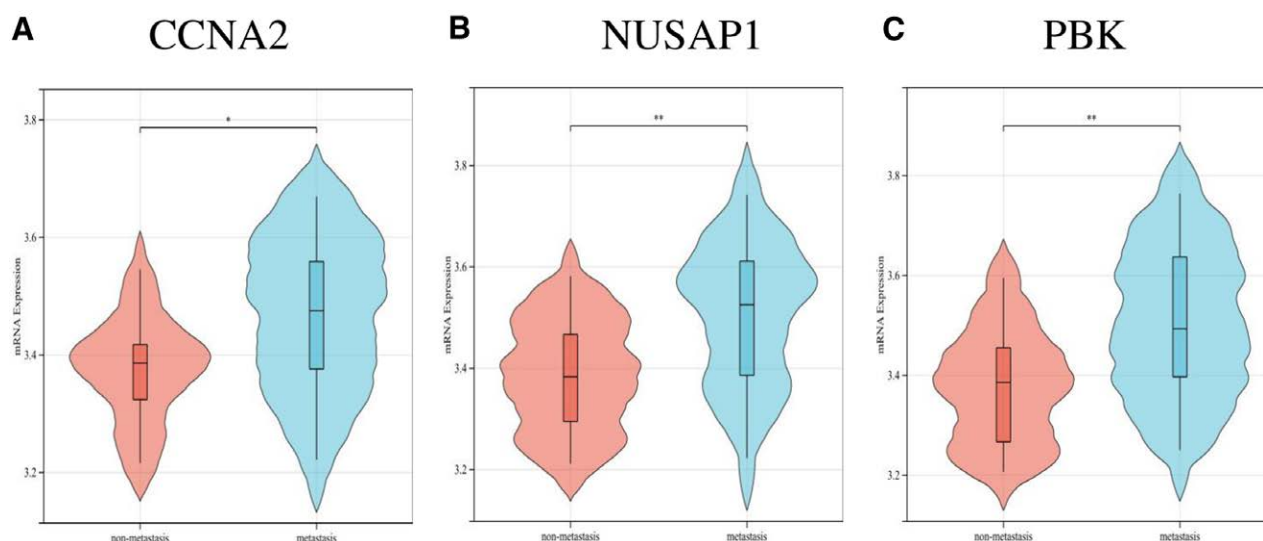


Figure 7. Gene expression validation (* < .05, ** < .01).

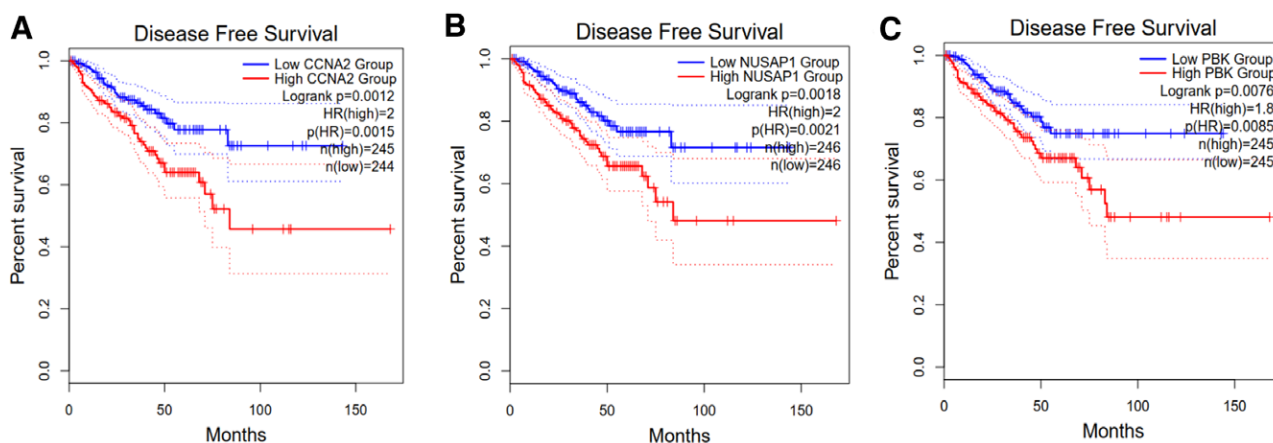


Figure 8. Based on Kaplan-Meier survival analysis in GEPIA2.

CCNA2, NUSAP1, and PBK expression might be associated with a lower survival rate (Fig. 8).

3.8. Infiltration analysis of immune cells

A total of 24 credible samples were obtained by the CIBERSORTx reverse convolution algorithm on the matrix with a screening criterion of $P < .05$. The stacked plot was used to illustrate the proportion of 22 immune cells in the primary and bone metastasis groups (Fig. 9A). A higher percentage of Treg cells and macrophages M0 were found in patients who had bone metastases from PCa (Fig. 9B). A positive correlation was observed between regulatory T cells (Tregs) and mast cells in bone metastasis samples ($R = 0.61$); the macrophages M0 were positively correlated with the follicular helper T cells ($R = 0.55$); however, the memory B cells were negatively correlated ($r = -0.57$) (Fig. 9C). The TIMER database was analyzed to correlate CCNA2, NUSAP1, and PBK with 6 major immune cells. Results indicated that CCNA2 and NUSAP1 were positively correlated with all 6 immune cells, CD4+ T cells had a negative correlation with PBK, but the other 5 immune cells had a positive correlation ($P < .05$) (Fig. 10).

4. Discussion

PCa is most commonly spread by bone metastasis,^[19] leading to debilitating complications that include pain, and pathological fractures.^[20] It's critical to underscore that the treatment of PCa becomes substantially challenging once it metastasizes to the bone, ultimately leading to its unfortunate demise,^[21] but there is still a lack of understanding of the precise molecular mechanisms underlying the immune microenvironment.^[22] This makes it imperative that new targets can be identified to facilitate early detection, potent therapies, and accurate prognosis of the immune microenvironment within PCa bone metastasis, thereby yielding substantial clinical benefits. In the recent past, advancements in gene expression analysis techniques, particularly microarray technology and high-throughput methods, have facilitated our study of the molecular mechanisms of complex diseases.

In this study, we screened and obtained 3 genes that are closely associated with PCa bone metastasis, namely CCNA2, NUSAP1, and PBK. The prospect of multi-biomarker combined detection is gaining traction as a promising strategy for improving cancer diagnosis and treatment. Utilizing a panel of biomarkers, including CCNA2, NUSAP1, and PBK, may enhance the sensitivity and specificity of cancer detection compared to

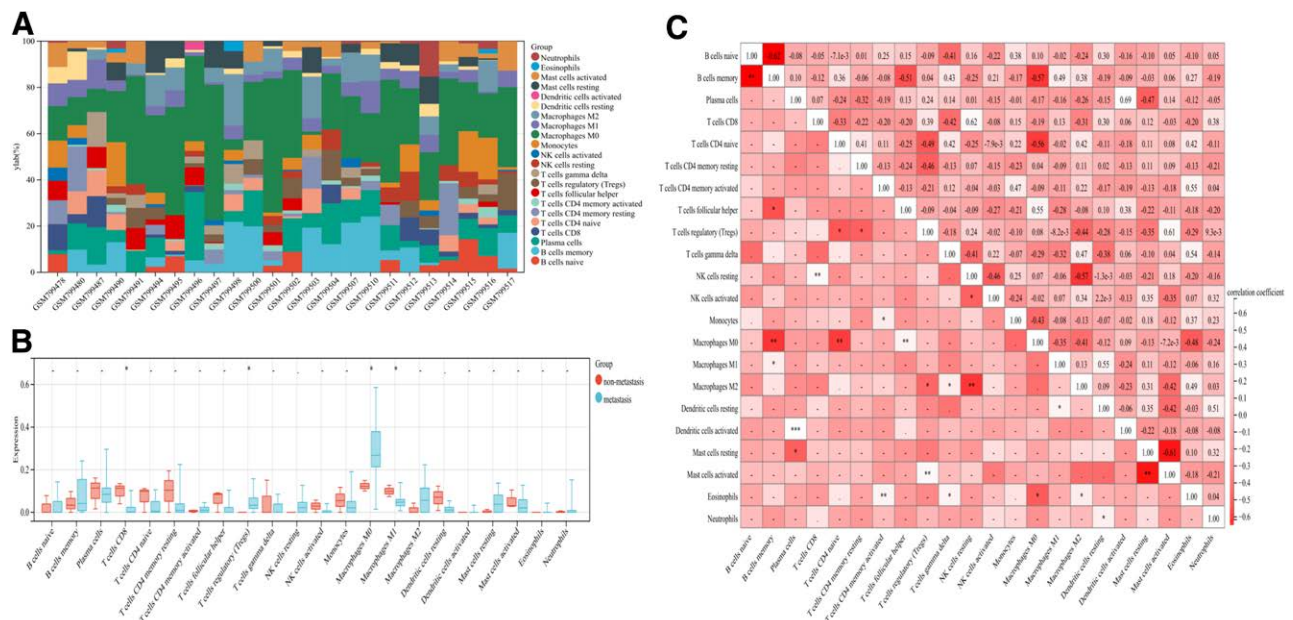


Figure 9. Analyzing and visualizing immune cell infiltration. (A) Different samples are represented by a bar graph showing the percentage of 22 immune cells; (B) immune cell infiltration in prostate cancer bone metastases versus primary prostate cancer; (C) correlation between 22 immune cells within prostate cancer bone metastases.

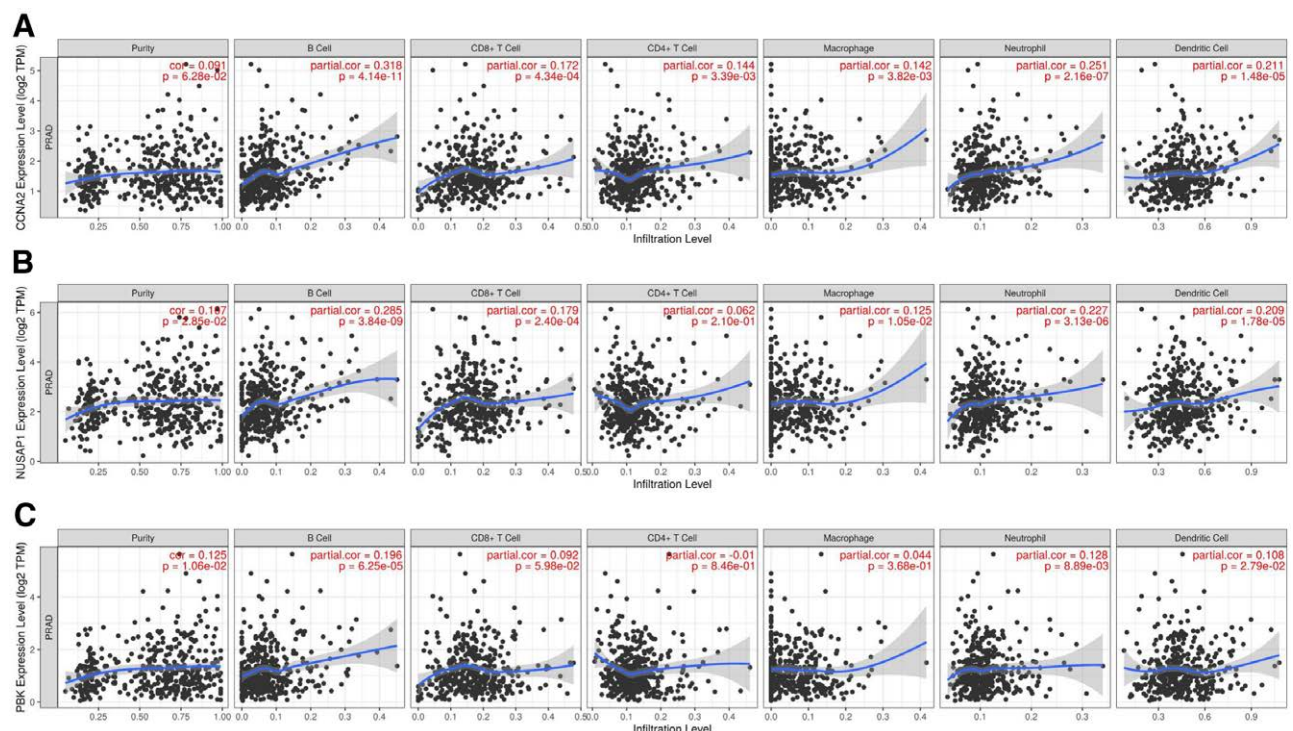


Figure 10. A scatter plot of 3 hub genes correlated with immune cells.

single biomarker approaches. For instance, studies have indicated that the simultaneous assessment of multiple biomarkers can provide a more comprehensive understanding of tumor heterogeneity and the underlying molecular mechanisms driving cancer progression.^[23,24]

The protein that CCNA2 encodes is a pivotal player in regulating cellular cycles. Accumulating data suggests an influential role of CCNA2 in accentuating cancer's invasiveness, recurrence, metastasis, and resistance to chemotherapy.^[25]

potentially through its participation in the epithelial-mesenchymal transition.^[26] Furthermore, results of the study have been introduced suggesting that CCNA2, operating as a cell cycle overseer, bolsters PCa invasion via modulation of metalloproteinases and VEGF expression and interaction with the androgen receptor.^[27] Research by Rui Yang^[28] demonstrated that small interfering RNA inhibited CCNA2 expression in PCa cell lines significantly reducing their ability to migrate and invade. Underscoring CCNA2's potential clinical relevance,

these results support its consideration as a therapeutic target for PCa.

NUSAP1, a nucleolar-spindle-associated protein, contributes to the organization of spindle microtubules. The proteins that interact with NUSAP1 have shown involvement in RNA binding, splicing, and transport, suggesting these pathways could be the primary promoters of cancer aggressiveness.^[29] This protein possibly promotes metastasis when it modulates FAM101B, an effector of TGF-1 signaling,^[30] TGFβ1 encourages invasion and metastatic progression in prostate tumors.^[31] This suggests that NUSAP1 could serve as a biomarker to track PCa progression.

According to a specific study, PBK expression correlates with metastatic capacity in PCa, this overexpression leads to an upregulation of matrix metalloproteinases-2 and -9, crucial contributors to metastatic invasion, which allow invading cells to enter the circulation by breaching endothelial barriers and basement membranes.^[32] The direct targeting of E2F1 by PBK in PCa cells has been demonstrated.^[33] Increasing expression of E2F1 may promote hormone-independent PCa by interfering with androgen receptor transcription. In this case, PBK may contribute significantly to distant metastasis of PCa in humans.^[34]

Investigations into the common regulatory mechanisms between PBK and NuSAP reveal that both proteins may converge on shared signaling pathways that govern cell proliferation and survival. PBK has been shown to drive tumorigenesis through transcriptional regulation of CCNB2, which is critical for cell cycle progression.^[35] Similarly, NuSAP's role in microtubule dynamics can influence cell cycle checkpoints and mitotic progression, suggesting that aberrations in their functions could lead to enhanced malignancy. Furthermore, studies indicate that PBK can modulate the p53 pathway, a pivotal tumor suppressor involved in cellular stress responses, thereby affecting autophagy and apoptosis in cancer cells.^[36] This intersection of regulatory mechanisms underscores the potential for PBK and NuSAP to be co-targeted in therapeutic interventions, particularly in cancers characterized by dysregulated cell cycle control and resistance to standard treatments.

Immune cell infiltration is shown to play a crucial role in tumor progression in the case of PCa.^[37] Using the CIBERSORTx deconvolution algorithm, we analyzed the wetting of 22 different immune cells in each sample. Our findings indicate that patients suffering from bone metastases linked to PCa demonstrate an escalated infiltration rate of Tregs and M0 macrophages.

Tregs infiltration may partially guide the immune response to primary tumor development, whether suppressive or stimulatory.^[38] One study confirms the presence of abundant Tregs in tumor tissues in cases of PCa, with their prevalence tightly linked to cancer severity and prognosis.^[39] By suppressing antitumor responses, Tregs induce tumor metastasis and migration.^[40] An animal model validates that intraperitoneal injection of anti-CCR10 immunotoxin hinders intratumoral Treg cell activity and thus reduces tumor expansion, showing a link between the growth of human malignancy and Treg cells.^[41]

M0 macrophages are plastic cells capable of phenotype alterations, potentially transitioning towards tumor-associated macrophages.^[42] Tumor-associated macrophages can foster tumor growth and treatment resistance via the secretion of cytokines and angiogenic mediators.^[43] Research by Caibin Fan et al.^[44] posited that a high concentration of M0 macrophages forecasts a deteriorating prognosis. The progression and recurrence of tumors in the prostate appear to be significantly influenced by tumor-associated macrophages, in particular M0 macrophages.^[45]

5. Conclusion

Considering the significance of Tregs and M0 macrophages in tumor expansion and metastasis, they could be crucial targets

for future immunotherapy strategies in patients battling PCa bone metastasis. Three hub genes, CCNA2, NUSAP1, and PBK, as well as 2 immune cell types, Tregs, and macrophages M0, were identified in this study as having good clinical research value in PCa bone metastasis through bioinformatics. We base all of our conclusions on a reanalysis of existing data, which can be verified by experiments in the future.

Acknowledgments

Thank the Gene Expression Omnibus database for the datasets GSE32269.

Author contributions

Conceptualization: Shu-Kun Lin.

Investigation: Chen-Ming Zhang.

Methodology: Zhong Hua.

Project administration: Si-Cheng Ma.

Writing – original draft: Fang Zhang.

Writing – review & editing: Bo Men.

References

- [1] Sung H, Ferlay J, Siegel RL, et al. Global cancer statistics 2020: GLOBOCAN estimates of incidence and mortality worldwide for 36 cancers in 185 countries. *CA Cancer J Clin.* 2021;71:209–49.
- [2] Tsuzuki S, Park SH, Eber MR, Peters CM, Shiozawa Y. Skeletal complications in cancer patients with bone metastases. *Int J Urol.* 2016;23:825–32.
- [3] Ye X, Huang X, Fu X, et al. Myeloid-like tumor hybrid cells in bone marrow promote the progression of prostate cancer bone metastasis. *J Hematol Oncol.* 2023;16:46.
- [4] Kabunda J, Gabela L, Kalinda C, Aldous C, Pillay V, Nyakale N. Comparing 99mTc-PSMA to 99mTc-MDP in prostate cancer staging of the skeletal system. *Clin Nucl Med.* 2021;46:562–8.
- [5] Jhunjhunwala S, Hammer C, Delamarre L. Antigen presentation in cancer: insights into tumour immunogenicity and immune evasion. *Nat Rev Cancer.* 2021;21:298–312.
- [6] Wu SQ, Su H, Wang YH, Zhao XK. Role of tumor-associated immune cells in prostate cancer: angel or devil? *Asian J Androl.* 2019;21:433–7.
- [7] Lopez-Bujanda Z, Drake CG. Myeloid-derived cells in prostate cancer progression: phenotype and prospective therapies. *J Leukoc Biol.* 2017;102:393–406.
- [8] Orlov YL, Anashkina AA, Klimontov VV, Baranova AV. Medical genetics, genomics and bioinformatics aid in understanding molecular mechanisms of human diseases. *Int J Mol Sci.* 2021;22:9962.
- [9] Song ZY, Chao F, Zhuo Z, Ma Z, Li W, Chen G. Identification of hub genes in prostate cancer using robust rank aggregation and weighted gene co-expression network analysis. *Aging (Albany NY).* 2019;11:4736–56.
- [10] Edgar R, Domrachev M, Lash AE. Gene expression omnibus: NCBI gene expression and hybridization array data repository. *Nucleic Acids Res.* 2002;30:207–10.
- [11] Shen W, Song Z, Zhong X, et al. Sangerbox: a comprehensive, interaction-friendly clinical bioinformatics analysis platform. *iMeta.* 2022;1:e36.
- [12] Subramanian A, Tamayo P, Mootha VK, et al. Gene set enrichment analysis: a knowledge-based approach for interpreting genome-wide expression profiles. *Proc Natl Acad Sci U S A.* 2005;102:15545–50.
- [13] Huang da W, Sherman BT, Lempicki RA. Systematic and integrative analysis of large gene lists using DAVID bioinformatics resources. *Nat Protoc.* 2009;4:44–57.
- [14] Szklarczyk D, Gable AL, Lyon D, et al. STRING v11: protein–protein association networks with increased coverage, supporting functional discovery in genome-wide experimental datasets. *Nucleic Acids Res.* 2019;47:D607–13.
- [15] Cerami E, Gao J, Dogrusoz U, et al. The cBio cancer genomics portal: an open platform for exploring multidimensional cancer genomics data. *Cancer Discov.* 2012;2:401–4.
- [16] Tang Z, Li C, Kang B, Gao G, Li C, Zhang Z. GEPIA: a web server for cancer and normal gene expression profiling and interactive analyses. *Nucleic Acids Res.* 2017;45:W98–W102.

- [17] Rusk N. Expanded CIBERSORTx. *Nat Methods*. 2019;16:577.
- [18] Li T, Fu J, Zeng Z, et al. TIMER2.0 for analysis of tumor-infiltrating immune cells. *Nucleic Acids Res*. 2020;48:W509–14.
- [19] Kfoury Y, Baryawno N, Severe N, et al. Human prostate cancer bone metastases have an actionable immunosuppressive microenvironment. *Cancer Cell*. 2021;39:1464–78.e8.
- [20] Coleman RE, Croucher PI, Padhani AR, et al. Bone metastases. *Nat Rev Dis Primers*. 2020;6:83.
- [21] Hofbauer LC, Bozec A, Rauner M, Jakob F, Perner S, Pantel K. Novel approaches to target the microenvironment of bone metastasis. *Nat Rev Clin Oncol*. 2021;18:488–505.
- [22] Arnold RS, Fedewa SA, Goodman M, et al. Bone metastasis in prostate cancer: Recurring mitochondrial DNA mutation reveals selective pressure exerted by the bone microenvironment. *Bone*. 2015;78:81–6.
- [23] Wang C, Zhang L. Bioinformatics-based identification of key genes and pathways associated with colorectal cancer diagnosis, treatment, and prognosis. *Medicine (Baltim)*. 2022;101:e30619.
- [24] Man YN, Xu H, Chen PJ, Sun Y, He ML. Comprehensive analysis of the clinical significance and molecular mechanism of T-box transcription factor 3 in osteosarcoma. *J Cancer*. 2024;15:4007–19.
- [25] Fischer M, Quaas M, Steiner L, Engeland K. The p53-p21-DREAM-CDE/CHR pathway regulates G2/M cell cycle genes. *Nucleic Acids Res*. 2016;44:164–74.
- [26] Bendris N, Arsic N, Lemmers B, Blanchard JM. Cyclin A2, Rho GTPases and EMT. *Small GTPases*. 2012;3:225–8.
- [27] Gomez LA, de Las Pozas A, Reiner T, Burnstein K, Perez-Stable C. Increased expression of cyclin B1 sensitizes prostate cancer cells to apoptosis induced by chemotherapy. *Mol Cancer Ther*. 2007;6:1534–43.
- [28] Yang R, Du Y, Wang L, Chen Z, Liu X. Weighted gene co-expression network analysis identifies CCNA2 as a treatment target of prostate cancer through inhibiting cell cycle. *J Cancer*. 2020;11:1203–11.
- [29] Stumpf CR, Ruggero D. The cancerous translation apparatus. *Curr Opin Genet Dev*. 2011;21:474–83.
- [30] Gordon CA, Gong X, Ganesh D, Brooks JD. NUSAP1 promotes invasion and metastasis of prostate cancer. *Oncotarget*. 2017;8:29935–50.
- [31] Jones E, Pu H, Kyprianou N. Targeting TGF-beta in prostate cancer: therapeutic possibilities during tumor progression. *Expert Opin Ther Targets*. 2009;13:227–34.
- [32] Brown-Clay JD, Shenoy DN, Timofeeva O, Kallakury BV, Nandi AK, Banerjee PP. PBK/TOPK enhances aggressive phenotype in prostate cancer via β -catenin-TCF/LEF-mediated matrix metalloproteinases production and invasion. *Oncotarget*. 2015;6:15594–609.
- [33] Chen JH, Liang YX, He HC, et al. Overexpression of PDZ-binding kinase confers malignant phenotype in prostate cancer via the regulation of E2F1. *Int J Biol Macromol*. 2015;81:615–23.
- [34] Davis JN, Wojno KJ, Daignault S, et al. Elevated E2F1 inhibits transcription of the androgen receptor in metastatic hormone-resistant prostate cancer. *Cancer Res*. 2006;66:11897–906.
- [35] Mao P, Bao G, Wang YC, et al. PDZ-Binding kinase-dependent transcriptional regulation of CCNB2 promotes tumorigenesis and radio-resistance in glioblastoma. *Transl Oncol*. 2020;13:287–94.
- [36] Park JH, Park SA, Lee YJ, Park HW, Oh SM. PBK attenuates paclitaxel-induced autophagic cell death by suppressing p53 in H460 non-small-cell lung cancer cells. *FEBS Open Bio*. 2020;10:937–50.
- [37] Dai J, Lu Y, Roca H, et al. Immune mediators in the tumor microenvironment of prostate cancer. *Chin J Cancer*. 2017;36:29.
- [38] Davidsson S, Andren O, Ohlson AL, et al. FOXP3(+) regulatory T cells in normal prostate tissue, postatrophic hyperplasia, prostatic intraepithelial neoplasia, and tumor histological lesions in men with and without prostate cancer. *Prostate*. 2018;78:40–7.
- [39] Miller AM, Lundberg K, Ozenci V, et al. CD4+CD25high T cells are enriched in the tumor and peripheral blood of prostate cancer patients. *J Immunol*. 2006;177:7398–405.
- [40] Hurwitz MD. Chemotherapy and radiation for prostate cancer. *Transl Androl Urol*. 2018;7:390–8.
- [41] Facciabene A, Peng X, Hagemann IS, et al. Tumour hypoxia promotes tolerance and angiogenesis via CCL28 and T(reg) cells. *Nature*. 2011;475:226–30.
- [42] Qiu SQ, Waaijer SJH, Zwager MC, de Vries EGE, van der Vegt B, Schröder CP. Tumor-associated macrophages in breast cancer: Innocent bystander or important player? *Cancer Treat Rev*. 2018;70:178–89.
- [43] Ruffell B, Coussens LM. Macrophages and therapeutic resistance in cancer. *Cancer Cell*. 2015;27:462–72.
- [44] Fan C, Lu W, Li K, et al. Identification of immune cell infiltration pattern and related critical genes in metastatic castration-resistant prostate cancer by bioinformatics analysis. *Cancer Biomark*. 2021;32:363–77.
- [45] Jairath NK, Farha MW, Srinivasan S, et al. Tumor immune microenvironment clusters in localized prostate adenocarcinoma: prognostic impact of macrophage enriched/plasma cell non-enriched subtypes. *J Clin Med*. 2020;9:1973.